Available online at www.sciencedirect.com
SCIENCE DIRECT
Polymer 46 (2005) 5992–6000
polymer
www.elsevier.com/locate/polymer

Single crystal morphology of star-branched polyesters with crystallisable poly(ε-caprolactone) arms

E. Núñez, U.W. Gedde*

Fibre and Polymer Technology, Royal Institute of Technology, SE-100 44 Stockholm, Sweden

Received 27 December 2004; received in revised form 11 April 2005; accepted 19 May 2005
Available online 14 June 2005

Abstract

Star-branched polymers consisting of poly(ε-caprolactone) (PCL) attached to third generation dendrimer, hyperbranched and dendron cores have been studied together with linear PCL analogues. The degree of polymerisation of the PCL arms of the star-branched polymers ranged from 14 to 81. Single crystals were grown from dilute solution and studied by transmission electron microscopy. Single crystals of linear PCL were multilayer hexagons with flat or slightly curved {110} and {100} faces. These single crystals were larger along [010] than along [100]. Single crystals of star-branched PCL showed the same basic shape, but with many crystallographic and irregular steps on the lateral crystal faces. The width of the micro-faces was typically 100–300 nm. These single crystals were more extended along [100] than along [010]. It is proposed that the high fold surface free energy and the constrained character of the star-branched polymers favour the formation of steps on the growth faces. Globular polycrystalline aggregates were also observed. They originated from a more concentrated polymer phase following phase separation of the solution. In the case of the star-branched polymers, lamellar branching was observed with a 30° angle between the crystals arms.

Keywords: Star-branched poly(ε-caprolactone); Single crystal; Transmission electron microscopy

1. Introduction

A star-branched polymer consists of a central core linking together three or more linear polymer chains. The star-branched polymers used in this study were based on three different dendritic cores (dendrimer, hyperbranched and dendron) with AB_2 monomers to which linear poly(ε-caprolactone) (PCL) is attached. The crystallisation, melting, crystal unit cell and crystalline superstructure of star-branched PCL have been extensively studied by Núñez et al. [1,2]. X-ray diffraction indicated that the star-branched polymers had the same crystal unit cell as linear PCL [1]. The crystallinity depression of the star-branched polymers with respect to linear PCL suggested that a few PCL repeating units close to the dendritic units were unable to crystallize and that the presence of the dendritic cores made the chain folds less tight [1]. Crystal rearrangement during the slow heating of samples previously crystallised during fast cooling occurred at a considerably lower rate in the star-branched polymers with dendrimer and hyperbranched cores [1]. The star-branched polymers had higher equilibrium melting points than their linear analogues, and this was explained as being due to a decrease in the melt entropy of the star-branched polymers with respect to the linear analogues, originating from the reduced positional freedom of the PCL arms of the star-branched polymers [1]. Star-branched polymers with PCL arms showed an unusual tendency to form spherulites, even when the PCL chains were very short [2]. The preference for spherulite formation was explained by the presence of dendritic core moieties on the fold surfaces that forced the branching lamellae to diverge and form spherulites in accordance with the scheme proposed by Bassett [3]. Linear PCL of similar molar mass crystallised dominantly in axialites, because ciliation was lacking and branching lamellae showed only a slight divergence. The crystallisation kinetics data suggested that the star-branched polymers have a higher fold surface energy than the linear polymers of the same PCL chain length, which confirms the effect of the dendritic cores on the fold surface [2].

* Corresponding author. Tel.: +46 8 790 7640; fax: +46 8 208 856.
E-mail address: gedde@polymer.kth.se (U.W. Gedde).

0032-3861/$ - see front matter © 2005 Elsevier Ltd. All rights reserved.
doi:10.1016/j.polymer.2005.05.083

This third paper in the series deals with the morphology of single crystals of star-branched PCL grown from dilute solution. There is, to our knowledge, nothing in the literature about the single crystal morphology of this class of polymers. Most studies [4–7] on semicrystalline star-branched polymers have reported melting point and crystallinity data without any detailed analysis of the morphology. Risch et al. [8], however, reported for melt-crystallized star-branched and linear polyamide-6 that the superstructure appeared to be unaffected by the molecular architecture, whereas the fine lamellar structure was more irregular in the star-branched polymers than in the linear analogues.

The single-crystal morphology of linear PCL has been described by Iwata et al. [9–11], Brisse and Marchessault [12] and Bittiger et al. [13]. The linear PCL single crystals are hexagonal, and they usually contain many layers originating from screw dislocations and with a typical crystal thickness of 10 nm [9–13]. The six lateral faces were identified by electron diffraction: four {110} faces and two {010} faces [10]. However, the angles between the faces are not consistent with this crystallographic assignment. Section 3 shows that angles between the faces suggest that the faces of the PCL single crystals are {110} (four) and {100} (two). Iwata and Doi [10] observed radial striations indicating non-uniform alignment of the crystal stems deviating from the normal to the fold surface. They suggested that lamellar single crystals consist of micro-crystals with different degrees of chain packing.

In this study, single crystals of linear PCL and of star-branched polymers with PCL arms have been grown from solution and examined by transmission electron microscopy and electron diffraction. The morphological characteristics of the crystals studied are reported and, in particular, the differences with regard to the lateral habit between linear PCL and star-branched PCL are highlighted. The morphological features of the polycrystalline aggregates obtained from crystallisation of more concentrated phases after phase separation of the solution are also reported.

2. Experimental

2.1. Materials

The star-branched polymers consisted of poly(ε-caprolactone) grafted to dendritic hydroxyl-functional cores. The cores used were a third-generation hyperbranched polyester with approximately 32 terminal hydroxyl groups (Boltorn, Perstorp AB, Sweden), a third-generation dendrimer with 24 hydroxyl groups and a third-generation dendron with 8 hydroxyl groups. The synthesis and characterization of the star-branched polymers have been described earlier [14,15]. The average degree of polymerization of the PCL arms ranged from 14 to 81 between the different samples. Linear PCL samples with the trade names Tone P300, P1270 and P1241, purchased from Union Carbide, USA, were studied as received. Molecular structure data of the polymers are presented in Table 1.

2.2. Preparation of single crystals

Two methods were used to prepare the single-crystal suspensions. The first was based on the so-called self-seeding method introduced by Blundell et al. [16]. If a single-crystal suspension is heated to a moderate temperature, the turbidity disappears indicating dissolution of the crystals. However, small centres survive and they allow the crystals to start growing upon further cooling. Using this method, crystallisation can be effectively controlled, yielding crystals uniform in size. In this study, 2.5 mg polymer was dissolved in 10 ml *n*-hexanol or *n*-butanol at 110 °C and kept at this temperature for 10 min. The solutions were cooled at a rate of 15 ± 3 °C h^{-1} to either 35 or 40 °C and allowed to crystallize at this temperature overnight. The process was repeated thrice, with the difference that the dissolution temperature was set to 100 °C. The suspensions were finally allowed to cool to room temperature. These conditions were similar to those used by Iwata and Doi [10] for low molar mass PCL. The method described above will be referred as M1. Hot-stage polarized microscopy (Leitz Ortholux POL BK II equipped with a Mettler Hot Stage FP 82HT controlled by a Mettler FP90 Central Processor) showed that part of the growth occurred at the isothermal temperature (35 or 40 °C) and the remaining crystallisation occurred during the cooling phase to room temperature. Liquid phase separation occurred only during the cooling phase to room temperature.

The second method used was in accordance with Bittiger et al. [13]. Samples weighing 50 mg were dissolved in 5 ml toluene at 75 °C and either 10 ml *n*-hexanol or *n*-butanol was then added. After the vials containing the solutions had cooled to room temperature, the content was poured into open recipients to allow evaporation of the solvent. At the onset of turbidity, the suspensions were recollected for storage. This method will be referred as M2. Hot-stage polarized microscopy showed that crystallisation occurred at room temperature, partly from the initial solution and partly during the course of evaporation of the solvent. Phase separation occurred during the later stages from the more concentrated polymer solution.

The crystal suspensions obtained by the two methods were dropped onto TEM carbon-film-coated copper grids. Filter paper was placed below the grids to absorb the excess of solvent. The grids were allowed to dry and then shadowed with Au–Pd in a vacuum evaporator. The angle between the metal source and the grid surface was between 5 and 15°.

2.3. Transmission electron microscopy

Transmission electron microscopy bright field observations were carried out with a Philips Tecnai 10 electron

Table 1
Nomenclature and characteristics of polymers studied

Group	Core	M_{core} (g mol^{-1})[a]	n_{arms}[b]	Sample code	n[c]	T_m^0[d] (K)
PCL_n	–	–	1	PCL_{17}	17 (1.2)	329
				PCL_{39}	39 (1.5)	342.4
				PCL_{117}	117 (1.4)	351.1
D_n	3rd-generation dendrimer	3006	24	D_{14}	14 (1.3)	331
				D_{42}	42 (1.3)	346.8
				D_{51}	51 (1.3)	349.7
HB_n	3rd-generation Boltorn	3607	32	HB_{51}	51 (1.3)	349.8
Don_n	3rd-generation dendron	1008	8	Don_{15}	15 (1.3)	330
				Don_{81}	81 (1.4)	353.5

[a] Molar mass of core calculated theoretically from the chemical formula.
[b] Number of PCL arms attached to core.
[c] Number average of the degree of polymerisation of the PCL arms (n), obtained by H NMR [15]. The values within parentheses show the polydispersity ($\bar{M}_w/\bar{M}_n$) obtained by size exclusion chromatography applying the universal calibration procedure. The values presented for the star-branched polymers are estimated from data for linear PCL polymerized under similar conditions.
[d] Equilibrium melting point data from Núñez et al. [1].

microscope operating at 80 kV. Digital images were recorded with a Megaview II digital camera and analyzed with the AnalySIS program after calibration with a patterned grid. Electron diffraction patterns were obtained from selected areas of single crystals.

3. Results and discussion

Hexagonal single crystals with slightly curved lateral faces, mostly multilayer and occasionally with a clearly visible central screw dislocation were the most common structure (Fig. 1; PCL_{39} single crystals grown from toluene/*n*-hexanol solution according to method M2). The lateral dimension of the single crystals was between 1 and 4 μm. These crystals had, according to hot-stage polarized microscopy, grown from a dilute solution environment. Electron diffraction patterns of single crystal type were only obtained from regions of thicker material including many crystal layers (Fig. 2). It was, however, possible to identify the direction of the crystallographic axes with respect to the lateral habit of the crystals in a few cases: the *b*-axis was along a vector between two corners of the crystal, each corner having an angle between the lateral faces of $113 \pm 3°$. The crystals were essentially symmetric about this vector. Iwata and Doi [10] observed linear PCL single crystals shaped as the crystals displayed in Fig. 1. However, they made a different assignment of the lateral faces of the single crystal,

A projection of the PCL crystal unit cell with the *a*- and *b*-axes in the plane is shown in Fig. 3. The unit cell parameter values used in the calculations are from Hu and Dorset [17]: $a = 0.748$ nm; $b = 0.498$ nm and $c = 1.726$ nm. In the left-hand side of the figure, the faces of the PCL single crystals are shown according to the assignment of Iwata and Doi [10]. The angle between the two {110} faces (α) is

Fig. 1. Transmission electron micrograph of PCL_{39} single crystals grown from toluene/*n*-hexanol solution according to method M2. The arrows indicate the crystallographic *b*-axis of the different single crystals.

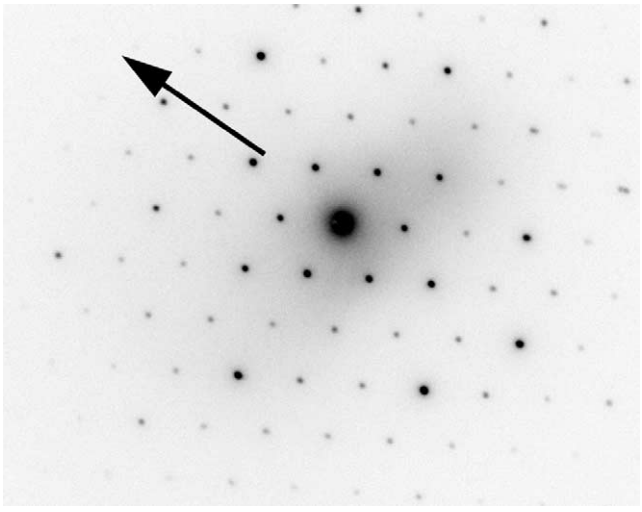

Fig. 2. Electron diffraction pattern taken of a selected area of a stack of crystal lamellae. The arrow indicate the direction of the crystallographic *b*-axis.

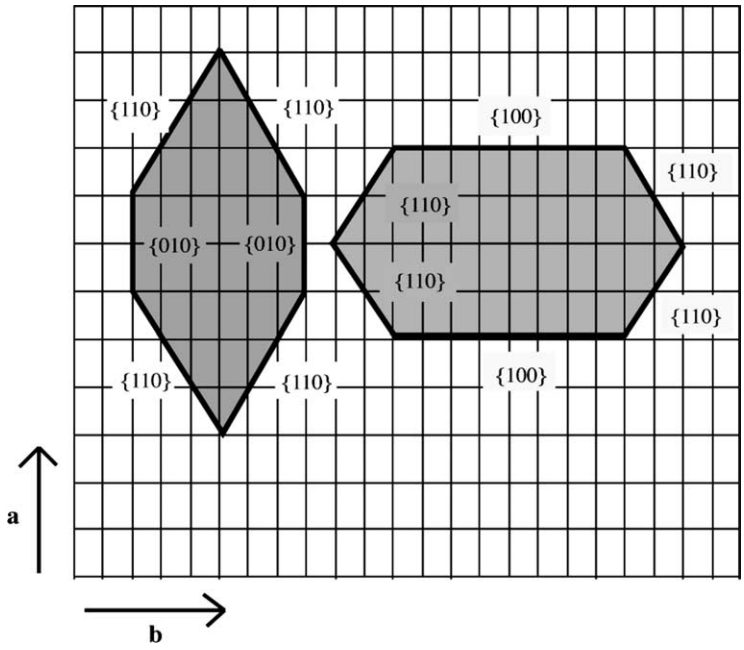

Fig. 3. Schematic drawing of an ensemble of PCL unit cells showing the *ab*-plane. The left-hand side shows the lateral faces of the single crystal according to Iwata and Doi [10]. The right-hand side shows an alternative assignment of the lateral faces.

calculated according to:

$$\alpha = 2\left(90 - \arctan\left(\frac{0.748}{0.498}\right)\right) \approx 68^\circ \quad (1)$$

The angle between the {110} and {010} faces (β) is given by:

$$\beta = 90 + \arctan\left(\frac{0.748}{0.498}\right) \approx 146^\circ \quad (2)$$

These angles are clearly inconsistent with the features of the PCL single crystals presented by Iwata and Doi [10] and with the shape of the crystals displayed in Fig. 1.

An alternative interpretation of the single crystal faces is shown in the right-hand part of Fig. 3. In this case, the angle (here denoted α') between the two {110} faces, is:

$$\alpha' = 2\left(90 - \arctan\left(\frac{0.498}{0.748}\right)\right) \approx 113^\circ \quad (3)$$

The angle between {100} and {110}, denoted β', is given by:

$$\beta' = 90 + \arctan\left(\frac{0.498}{0.748}\right) \approx 124^\circ \quad (4)$$

The angles between the single crystal faces displayed in the micrographs presented by Iwata and Doi [10] are $110 \pm 5^\circ$ and $125 \pm 5^\circ$. These angle are thus consistent with the following reinterpretation of the single crystal faces: four {110} faces and two {100} faces. Hence, the {110}–{110} tip is along the crystallographic *b*-axis. The lateral habit of the PCL single crystals resembles that of linear polyethylene with almost the same dimensions of the unit cell in the *ab* plane: $a = 0.741$ nm and $b = 0.495$ nm [18]. The predicted angles for linear polyethylene between two {110} and between the {110} and {100} faces are, respectively, 113 and 124°, i.e. the same values as obtained for PCL. Six-sided linear polyethylene single crystals grown from xylene solution at 90 °C showed the angles 113 and 125° [19], i.e. close to the theoretical values. This interpretation further means that the regular chain folding in linear PCL would be the same as for linear polyethylene. i.e. along [110] and [010].

Polycrystalline globular aggregates resembling spherulites obtained after bulk crystallisation were occasionally observed (Fig. 4; Don_{81} crystallised from toluene/*n*-hexanol solution according to method M2). These aggregates was found in samples crystallized according to both methods (M1 and M2). The spherical shape of these crystal aggregates suggests an origin in a minor, polymer-rich phase. Hence, these structures could exist only in a solution that had undergone phase separation. Schaaf et al. [20] observed globular crystalline morphologies grown in solutions using poor solvents. Polarized microscopy showed that phase separation occurred late after the growth of the single crystals during or after cooling from the isothermal crystallisation temperature. Fig. 5 shows a polycrystalline aggregate of D_{42} crystallised from toluene/*n*-hexanol solution according to method M2. A more detailed examination of the spherical crystal aggregates revealed crystals radiating from the centre (Fig. 5). Continuity and branching of the lamellae were observed with an angle of 30° between the branching crystal arms (Fig. 5). This is consonant with the picture for other spherulite-forming polymers such as polyethylene of sufficiently high molar

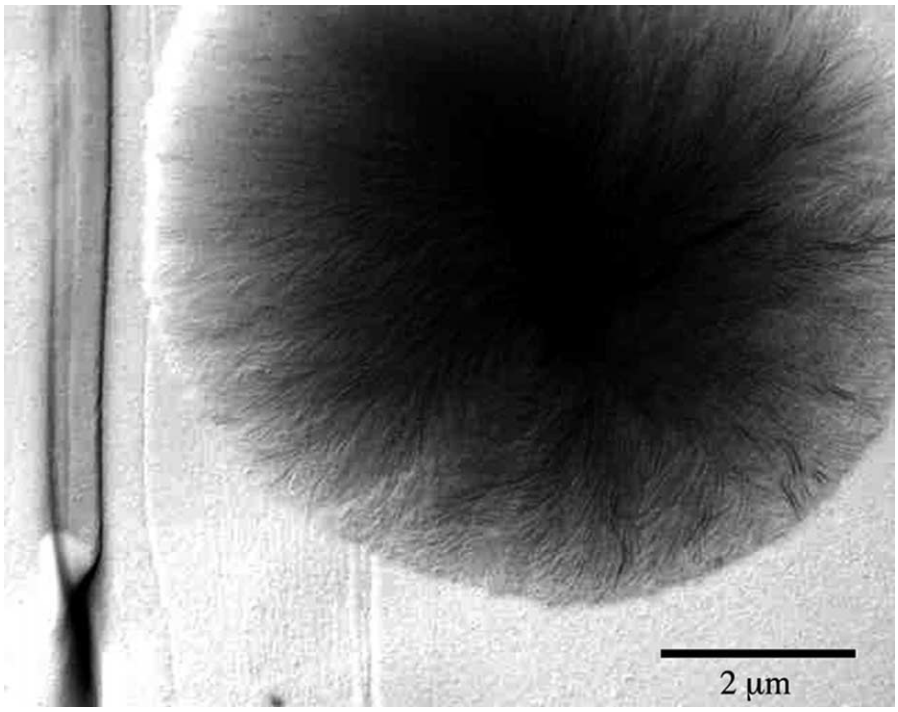

Fig. 4. Transmission electron micrograph of a polycrystalline aggregate of Don_{81} crystallised from toluene/*n*-hexanol solution according to method M2.

mass [3]. The branching and splaying of the crystal lamellae in the globular polycrystalline aggregates of the star-branched polymers is also in accordance with the great ability of these polymers to form spherulites [2].

Fig. 6 shows single crystals of PCL_{17} grown at 40 °C from *n*-hexanol solution according to method M1. These single crystals showed almost perfect six-sided facetted crystals with four {110} faces and two {100} faces. The angle between two adjacent {110} faces was $112 \pm 2°$, which is close to the theoretical value of 113°. The angle between the {110} and {100} faces was $125 \pm 3°$, which is close to the theoretical value of 124°. The lateral faces were flat without steps or niches. The length of the crystals along [010] (l_b) was approximately twice that along [100] (l_a). The single crystals of the higher molar mass PCL_{39} were hexagons with four {110} faces and two {100} faces (Fig. 1). The lateral faces were slightly rounded. The angles between the two adjacent {110} faces were within the range $111 \pm 3°$ and the angles between {110} and {100} were approximately 125°. Some crystals showed a more pronounced curvature. Rare examples of {100} steps on {110} faces were found (Fig. 1). The crystal shape was less

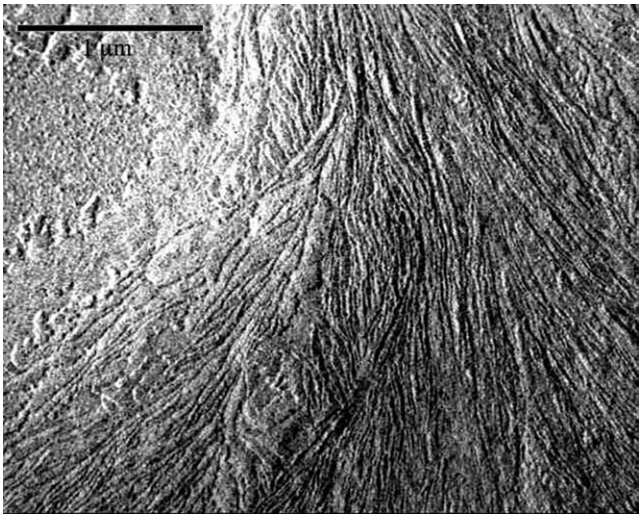

Fig. 5. Transmission electron micrograph of a polycrystalline aggregate of D_{42} crystallised from toluene/*n*-hexanol solution according to method M2.

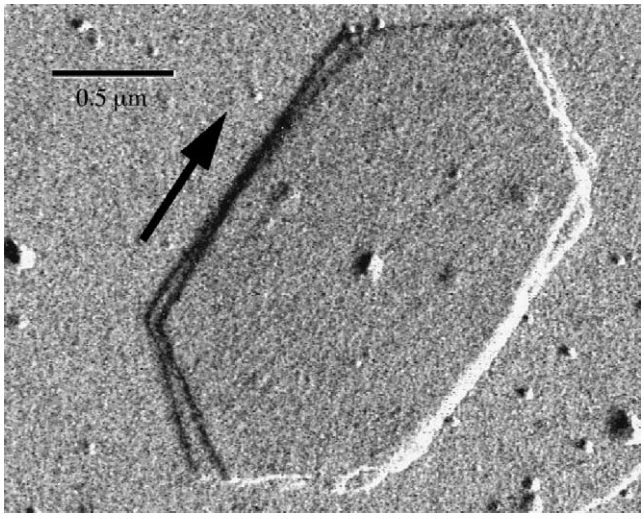

Fig. 6. Transmission electron micrograph of PCL_{17} single crystals grown at 40 °C from *n*-hexanol solution according to method M1. The arrow indicates the direction of the crystallographic *b*-axis.

anisotropic than that of PCL_{17}: $l_b/l_a = 1.3–1.6$. Radial striations were observed in the {110} sectors (Fig. 1). Striations running perpendicular to the growth faces of polymer crystals have been observed before in PCL and other related polyesters [10,21,22]. Iwata and Doi [10] suggest that the striations are due to the presence of micro-crystals, 40 nm wide and 200–300 nm long oriented along the growth direction. Pouget et al. [22] detected striations in the more developed {110} sectors of hexagonal crystals of poly(tetramethylene adipate) and they proposed that the striations originated from the non-planar structure of the crystals. The striations were observed in single crystals of both linear and star-branched PCL and it thus seems that the underlying reason for their appearance is not the possible large difference in fold surface structure of the two classes of polymers.

Fig. 7 shows several good examples of pairs of left- and right-handed screw dislocations in single crystals of PCL_{39} grown from toluene/*n*-hexanol solution according to method M2. This feature was also observed in samples of the star-branched polymers.

The star-branched polymers showed single crystals different in several aspects from those of linear PCL. The lowest molar mass dendrimer PCL (D_{14}) showed six-sided single crystals with crystallographic angles. The crystals were more extended along [010] than along [100]: $l_b/l_a = 1.5–1.6$. One difference from the linear PCL single crystals was the presence of the great many {100} faces (steps) on the {110} faces. The micro-faces were typically 100–300 nm wide. Dendrimer PCL with longer PCL arms (D_{42}) showed the basic six-sided form with a more pronounced curvature and even more frequently occurring steps (Fig. 8; crystals grown from toluene/*n*-hexanol solution according to method M2). Some steps followed crystallographic planes whereas others were irregular. Figs. 9 and 10 show single crystals of HB_{51}, respectively, Don_{81} grown from toluene/*n*-hexanol solution according to method M2. The single crystals of these star-branched polymers showed essentially the same characteristics as those of D_{42}. The l_b/l_a ratio for the star-branched polymers with longer PCL arms was less than unity, i.e. the crystals showed faster growth along [100] than along [010]. Many of these crystals showed flat {100} faces with a width in the range of 150–400 nm (Figs. 8–10). The other four faces of these single crystals showed curvature, steps and niches. Some of the steps were between crystallographic planes, {100} faces (steps) on {110} faces whereas other appeared to be more irregular. These micro-faces were of the order of 100 nm in some cases (Figs. 8 and 9) and wider in other cases (Fig. 10).

Fig. 11 summarizes the crystal shape (l_b/l_a) data as a function of molecular architecture and degree of polymerisation of the PCL arms. It must be emphasized that the crystallisation temperature varied among the different samples. Polarized microscopy showed that crystallisation according to method M1 occurred during the isothermal phase (35 or 40 °C) or at lower temperatures during the cooling stage. Method 2 resulted in crystallisation at room temperature. Different solvents were also used, so that the degree of undercooling was not the same for the different samples. It is known from the systematic study of linear polyethylene by Organ and Keller [23] that the lateral habit changes with the absolute temperature of crystallisation. One feature common to both linear and star-branched PCL was that the l_b/l_a ratio decreased with increasing molar mass of the PCL arms (Fig. 10). The l_b/l_a ratio was significantly greater for linear PCL than for star-branched PCL Thus, growth by crystal re-entry along [010] rather than by re-entry along [110] occurred more frequently in the star-branched polymers than in linear PCL. This may be due to the constrained state of the star-branched polymers, but the

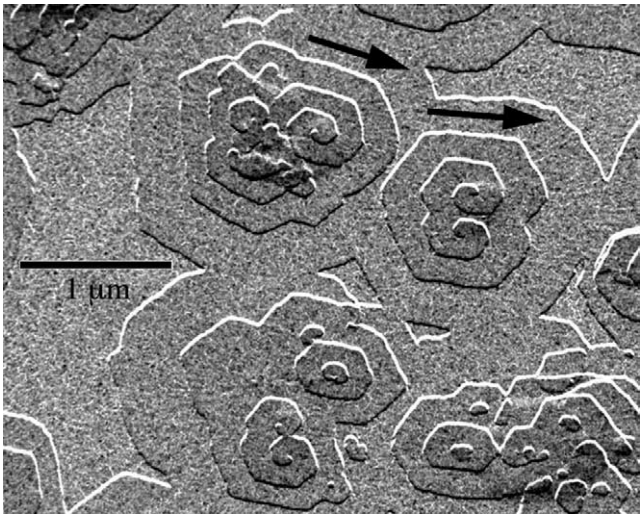

Fig. 7. Transmission electron micrograph of PCL_{39} single crystals grown from toluene/*n*-hexanol solution according to method M2. Arrows indicate screw dislocations of different handedness.

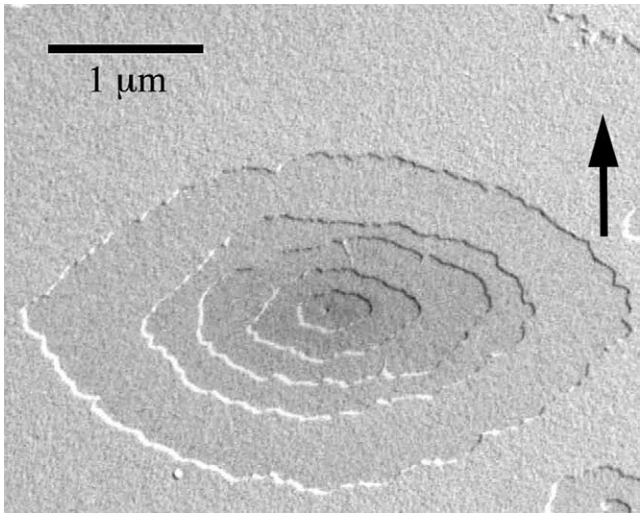

Fig. 8. Transmission electron micrograph of single crystals of D_{42} grown from toluene/*n*-hexanol solution according to method M2. The arrow indicates the direction of the crystallographic *b*-axis.

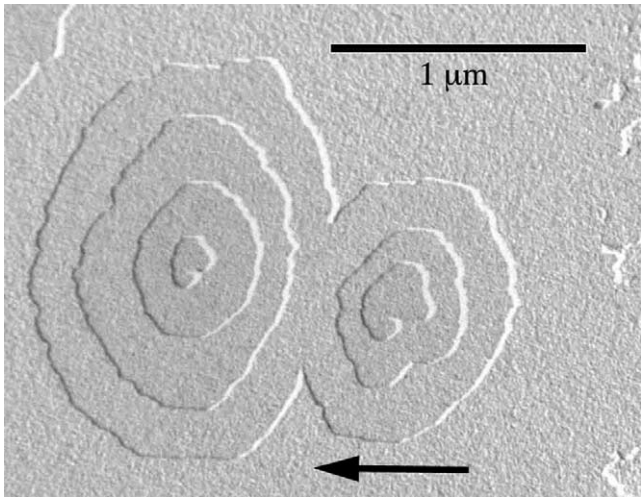

Fig. 9. Transmission electron micrograph of single crystals of HB_{51} grown from toluene/*n*-hexanol solution according to method M2. The arrow indicates the direction of the crystallographic *b*-axis.

implication that there was a lack of control of the crystallisation temperature cannot be ruled out.

Extremely curved faces were observed in crystals of a few star-branched PCL samples, especially in those with the longest PCL arms. Fig. 12 shows single crystals of Don_{81} with extremely curved growth faces. The crystals were grown at 40 °C from *n*-hexanol solution according to method M1. The lateral habit of the top crystal layer on the large rounded base layer was interestingly facetted with almost straight edges. Polyethylene shows a systematic change in lateral habit with respect to crystallisation temperature [23]: Crystals grown at higher temperatures become elongated along the crystallographic *b*-axis and show progressively more curvature on the {100} faces.

The difference in lateral habit between linear and star-branched PCL single crystals may be interpreted by using the Lauritzen–Hoffman scheme. Irregular lateral faces with only narrow regular micro-faces were the characteristic feature of the single crystals of the star-branched polymers whereas single crystals of linear PCL showed wide regular lateral faces. This difference in structure can be attributed to differences in the balance between the rate of nucleation of a new stem on the lateral smooth face (S) and the rate of lateral crystal growth (g). The nucleation rate is according to Lauritzen and Hoffman [24] given by:

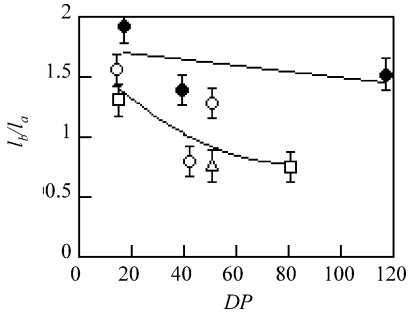

Fig. 11. Crystal shape factor (l_b/l_a) as a function of the degree of polymerisation (DP) of the PCL arms for linear PCL (●), dendrimer PCL (○), dendron PCL (□) and hyperbranched PCL (△) single crystals.

$$S = \beta N_0 \exp\left(-\frac{2bL_c\sigma_L}{RT} + \frac{\psi abL_c\Delta g}{RT}\right) - \beta N_1 \exp\left(-\frac{(1-\psi)abL_c\Delta g}{RT}\right) \quad (5)$$

where β is the rate of short-range diffusion of the crystallizable units, b is the thickness of the crystal monolayer, L_c is the crystal thickness, R is the gas constant, T is the temperature, ψ is a factor between 0 and 1, a is the crystal stem width, Δg is the change in free energy on

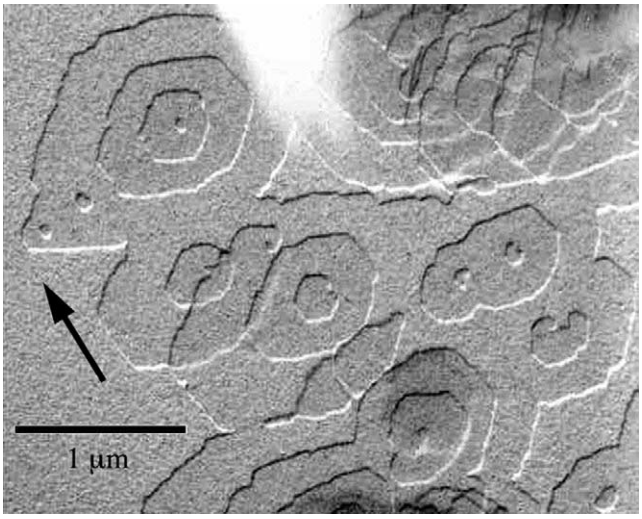

Fig. 10. Transmission electron micrograph of single crystals of Don_{81} grown from toluene/*n*-hexanol solution according to method M2. The arrow indicates the direction of the crystallographic *b*-axis.

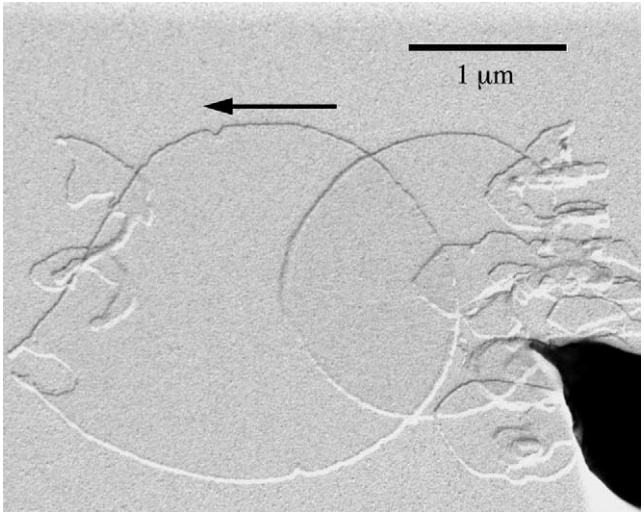

Fig. 12. Transmission electron micrograph of single crystals of Don_{81} crystallised at 40 °C from *n*-hexanol solution by method M1. The arrow indicates the direction of the crystallographic *a*-axis.

crystallisation, and N_0 and N_1 is the occupation number for zero and one stems, respectively. These quantities should be the same for linear and star-branched PCL except for Δg; the latter can be approximate by $\Delta h^0 \Delta T/T_m^0$ (Δh^0 is the heat of fusion, ΔT is the degree of supercooling and T_m^0 is the equilibrium melting point). There is an uncertainty in the precise temperature of crystallisation for the different samples and also in the degree of undercooling. The difference in equilibrium melting point between linear and star-branched PCL with the same molar mass of the crystallizable PCL units is typically 3–4 °C (higher for the star-branched polymers) [1]. Hence, the nucleation rate would be greater for the star-branched polymers than for linear PCL on crystallisation at a certain, specific temperature like in the case of method M1. It is possible that method M2 resulted in crystallisation at slightly different temperatures for the different samples with less variation in ΔT than in the case of method M1. The lateral growth rate is given by [24]:

$$g = a\beta\left(\exp\left(-\frac{2ab\sigma}{RT} + \frac{\psi abL_c\Delta g}{RT}\right) - \exp\left(-\frac{(1-\psi)abL_c\Delta g}{RT}\right)\right) \quad (6)$$

where σ is the specific fold surface free energy. Data for σ were obtained from measurements of the kinetics of melt-crystallisation of linear and star-branched PCL [2]: σ is larger by 30% for star-branched PCL than for linear PCL at a DP of 80–100. This percentage difference is even larger for polymers with shorter PCL arms [2]. The lateral growth rate (g) should then be lower for the star-branched polymers because of their higher fold surface energies than the linear polymers provided that the other quantities in Eq. (6) remain unchanged. It may be concluded that the higher fold surface free energy of star-branched PCL alters the balance between S and g. The ratio S/g should thus be larger for star-branched PCL than for linear PCL leading to more narrow micro-faces for the former group. The result of this qualitative analysis is thus in accordance with the observations made by transmission electron microscopy.

Another possible reason for the greater number of steps and niches in the single crystals of the star-branched polymers is attributed to their 'constrained' structure. A single star-branched polymer molecule makes 8 (dendron core), 24 (dendrimer core) or 32 (hyperbranched core) crystal entries from the core side of the molecule. The surface energetics may strive towards a smooth surface and this is more easily accomplished with a linear polymer molecule. The crystallizable PCL arms of the star-branched molecules have restricted mobility. Assume that a certain section of the star-branched molecule adds to the crystal (Fig. 13). The remaining part is then sticking out from the crystal. The other PCL arms cannot in this example make any further addition to complete the substrate. Instead, they may start an outgrowth in another crystallographic direction. The two dominant fold structures of PCL, according to the basic lateral habit, are along the directions [110] and [010]. Thus the start of a new direction for crystal re-entry may be the only possible way in which other PCL arms can be added to the single crystal.

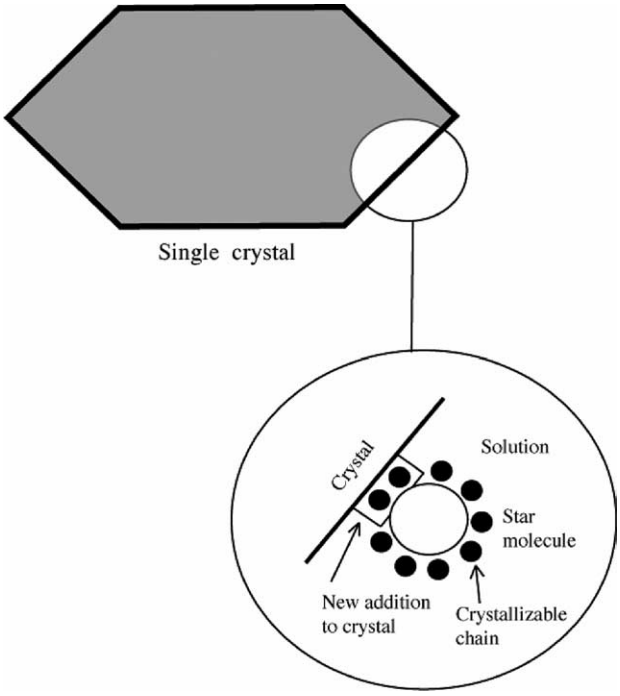

Fig. 13. Schematic drawing showing the addition of a star-branched molecule to a flat crystal substrate.

4. Conclusions

Single crystals of linear PCL and star-branched PCL grown from dilute solution have been studied by bright-field transmission electron microscopy and electron diffraction. A single crystal with six lateral sides (four {110} faces and two {100} faces) was the basic structure found. The majority of the hexagonal crystals were multilayer occasionally with a central screw dislocation. The spiral growth was both right- and left-handed, sometimes in the same crystal. Radiating striations in the {110} sectors were observed in single crystals of both linear and star-branched polymers. Linear PCL showed slightly curved crystals with only a few steps or niches and with the fastest growth direction along [010]. The star-branched polymers showed relatively flat {100} faces and large {110} faces with a great many steps and niches. Some of steps were crystallographic, i.e. a {110} face followed by a {010} face, which in turn was followed by a {110} face. Some of the steps and niches appeared to be irregular. The fastest growth direction of the single crystals of the star-branched polymers was [100], which suggest that re-entry along [010] was more favoured in these polymers than in linear PCL. The higher fold

surface energy of the star-branched polymers favour surface nucleation relative to the lateral crystal growth, which then leads to narrow crystal micro-faces. In addition, the constrained character of star-branched polymer molecules on the one hand and their non-planar shape on the other hand are other reasons for the many steps on the lateral faces. The use of another crystallographic direction for crystal re-entry may thus be more compatible with the geometry of the molecule.

Spherical polycrystalline aggregates were observed in the star-branched polymers. These are formed in a polymer-rich phase, after phase separation of the solution. The profound ability of the star-branched polymers to form spherulites even in the case of polymers with short PCL arms is consistent with the observations made by electron microscopy. The spherical aggregates consisted of a large number of radiating crystal lamellae with lamellar branching. The angle between branching lamellae was typically $\sim 30^{\circ}$. It is suggested that the core of the star-branched polymer is located at the fold surface and that the incompressibility of this structure causes the lamellae to diverge.

Acknowledgements

The financial support from the Swedish Research Council (grant # 5104-20005764/20) is gratefully acknowledged. Thanks are extended to Drs E. Malmström and H. Claesson, at our Department, for supplying the star-branched polymers, Dr M. Hedenqvist for discussions and experimental assistance and Dr B. Lotz, Institute Charles Sadron, Strasbourg, for valuable advice and discussions.

References

[1] Núñez E, Ferrando C, Malmström E, Claesson H, Werner PE, Gedde UW. Polymer 2004;45:5251.
[2] Núñez E, Ferrando C, Malmström E, Claesson H, Gedde UW. J Macromol Sci Phys 2004;43:1213.
[3] Bassett DC. CRC Crit Rev 1984;12:97.
[4] van Caeter P, Goethals EJ. Macromol Rapid Comm 1997;18:393.
[5] Chen E-Q, Lee S-W, Zhang A, Moon B-S, Mann I, Harris FW, et al. Macromolecules 1999;32:4784.
[6] Wei HY, Shi WF, Nie KM, Shen XF. Polymer 2002;43:1969.
[7] Zhao YL, Cai Q, Jiang J, Shuai XT, Bai JZ, Chen CF, et al. Polymer 2002;43:5819.
[8] Risch BG, Wilkes GL, Warakomski JM. Polymer 1993;34:2330.
[9] Iwata T, Doi Y. Macromol Chem Phys 1999;200:2429.
[10] Iwata T, Doi Y. Polym Int 2002;51:852.
[11] Iwata T, Furuhashi Y, Su F, Doi Y. RIKEN Rev 2001;42:15.
[12] Brisse F, Marchessault RH. ACS Symp Ser 1980;141:267.
[13] Bittiger H, Marchessault RH, Niegisch WD. Acta Crystallogr B: Struct Crystallogr Cryst Chem 1970;26:1923.
[14] Ihre H, Hult A, Söderlind E. J Am Chem Soc 1996;118:6388.
[15] Claesson H, Malmström E, Johansson M, Hult A. Polymer 2002;43: 3511.
[16] Blundell DJ, Keller A, Kovacs AJ. J Polym Sci, Polym Lett 1966;4: 481.
[17] Hu H, Dorset DL. Macromolecules 1990;23:4604.
[18] Busing WR. Macromolecules 1990;23:4608.
[19] Bassett DC, Frank FC, Keller A. Phil Mag 1963;8:1753.
[20] Schaaf P, Lotz B, Wittmann JC. Polymer 1987;28:193.
[21] Furuhashi Y, Sikorski P, Atkins E, Iwata T, Doi Y. J Polym Sci, Polym Phys 2001;39:2622.
[22] Pouget E, Almontassir A, Casas MT, Puiggala J. Macromolecules 2003;36:698.
[23] Organ SJ, Keller A. J Mater Sci 1985;20:1571.
[24] Lauritzen Jr JI, Hoffman JD. J Appl Phys 1973;44:4340.